Influence of Diethylene Glycol Content on Behavior of Poly(ethylene Terephthalate) Fibers

JIŘÍ MILITKÝ, JIŘÍ VANÍČEK,* JAN DOSTÁL, JAROSLAV JANSA, and JAROSLAV ČÁP, *Research Institute for Textile Finishing, 55428 Dvůr Králové nad Labem, Czechoslovakia*

Synopsis

Relationship between structural parameters of poly(ethylene terephthalate) (PET) fibers, their mechanical properties, and nonisothermal sorption of disperse dyes are investigated. Influence of diethylene glycol (DEG) addition and small changes in draw ratio are studied. Mechanical properties are characterized by stress–strain curves at constant deformation rate. The stress–strain relationships are described by means of derivative analysis. For treatment of nonisothermal experiments a simple kinetic model is suggested enabling to determine activation parameters of sorption. Further, the influence of a blank dye bath on the structure and properties of PET fibers is studied.

INTRODUCTION

One of the main criteria affecting applicability of PET fibers is their uniform dyeability. The literature states many factors that influence sorption properties of polymeric fibers. However, it is extremely difficult to correlate modifications in structure of the fibers with modifications in dyeing properties in a quantitative way.[1,17] Several publications describe how to correlate structural[3] and mechanical properties of PET fibers[2,8] with their sorption behavior. It is assumed, based on the experimentally proved hypothesis, that the rate of dye sorption in the PET fibers is a process dependent upon segmental mobility of chains in noncrystalline regions.[20]

On the basis of this hypothesis and the free-volume model of diffusion, relationships have been postulated between chosen technological parameters in fiber production and their dyeability.[21,22] However, little attention has been paid to the effect of diethylene glycol (DEG) on mechanical and sorption properties of PET fibers.[18] It is worth noting that the content of DEG produced during the polycondensation represents, due to side reactions, about 1–2 wt %.[15,15] DEG is a modifying component mostly bonded to macromolecular chains.[23] It stands to reason that irregular bonding of DEG in PET will adversely influence the uniformity of dyeing. The purpose of this study is to determine the effect of DEG on structure, mechanical behavior, and sorption properties of PET fibers. Further, the influence of practical dyeing conditions on structure of the fibers with different DEG content was examined.

* Present address: Chemopetrol–Silon Combine, Research Department, Planá nad Lužnicí, Czechoslovakia.

Journal of Applied Polymer Science, Vol. 25, 1195–1208 (1980)

0021-8995/80/0025-1195$01.40

EXPERIMENTAL

Material

The PET material was prepared on a laboratory scale by a discontinuous method. The increase of DEG content was achieved by adding pure DEG into the reaction mixture. The polymer was prepared without addition of DEG (samples I), with 1 wt % (samples II) and with 4% DEG (samples III). The wt % corresponds to initial quantity of dimethylterephthalate. The real content of DEG determined analytically was 0.87% in samples I, 1.17% in samples II, and 3.05% in samples III.

Spinning was performed on a laboratory spinning machine at 266°C dosing 9.8 g melt/min, spinning speed 300 m/min with two-stage drawing in aqueous bath at 70 and 90°C. One-half of the samples were drawn to an optimal drawing degree (marked 1), the second half to the degree 0.4 smaller (marked 2). All the samples were annealed in the relaxed state at 130°C for 20 min.

Structural Parameters of Fibers

Thermal Analysis. The samples were analyzed on a differential calorimeter DSC-1B. Melting point T_m (°C) was determined from the heating curve by a standard method.[4] From the position of the bend on the DSC curve in the exothermal direction (above the glass transition temperature), the so-called apparent setting temperature T_{rc} (°C) was determined characterizing the thermal history of the polymer.[4]

Density. Densities ρ were measured with a density gradient column containing a mixture of n-heptane and carbon tetrachloride at 30°C. From the values obtained, the volumetric crystallinity degree was determined as follows:

$$X = \frac{\rho - \rho_a}{\rho_c - \rho_a}$$

where $\rho_c = 1.455 \times 10^3$ kg/m^3 is the density of crystalline phase and $\rho_a = 1.33 \times 10^3$ kg/m^3 the density of amorphous phase.[5,6]

Orientation. To characterize overall orientation of the samples, birefringence Δn was determined on a polarization microscope with a Berek compensator. To assess orientation of the crystalline phase, a WAXD analysis was applied. From orientation of the normal to the (100) plane, the orientation factor of the crystalline phase f_c was determined by means of a classical method.[7] The orientation factor of the amorphous phase f_{am} was computed from the equation[11]

$$\frac{\Delta n}{X f_c} = \Delta^0 n_c + \Delta^0 n_{am} \left(\frac{1 - X}{X} \right) \frac{f_{am}}{f_c}$$

where $\Delta^0 n_c = 0.22$ is the intrinsic birefringence of the crystalline phase and $\Delta n_{am}{}^0 = 0.275$ the intrinsic birefringence of the amorphous phase.

Mechanical Properties

Stress–strain relationship at 25°C and rate of deformation $d\epsilon/dt = 1.66 \times 10^{-3}$ 1(sec^{-1}) were determined on the Instron testing machine with a test length of 10 mm. All values were determined as the mean of 50 curves.

Deformation ϵ, stress σ, modulus m = $d\delta/d\epsilon$ and deformation work d = $\epsilon d\epsilon$ were assessed at two characteristic points by means of derivative analysis[19]. The first point denotes the end of "pseudo-Hookean region" of deformation (subscript 1) corresponding to the maximum value of the modulus. The second point corresponds to the post yield point and thus to the beginning of the strain "softening" (subscript 2) and is indicated by the minimum value of the modulus (see Fig. 1). Further, values for σ_b, ϵ_b, and d_b were determined at the break point.

Dyeing. Pallanilblau 3RG (Disperse Blue 129) was used to study nonisothermal dyeing kinetics. The time–temperature course of dyeing is shown in Figure 2. The rate of heating in the nonisothermal region was 2°C/min (I). The dye bath, adjusted to pH 5 with acetic acid and amonium sulfate, contained 2% o.w.f. dye. Dyeing was carried out using an exhaustion method on a laboratory dyeing apparatus Linitest at a liquor ratio of 25:1. After completion of dyeing (i.e., after periods of 10, 20, 30, 40, 50, 60, 70, 80, 90, 120, and 150 min) the mean

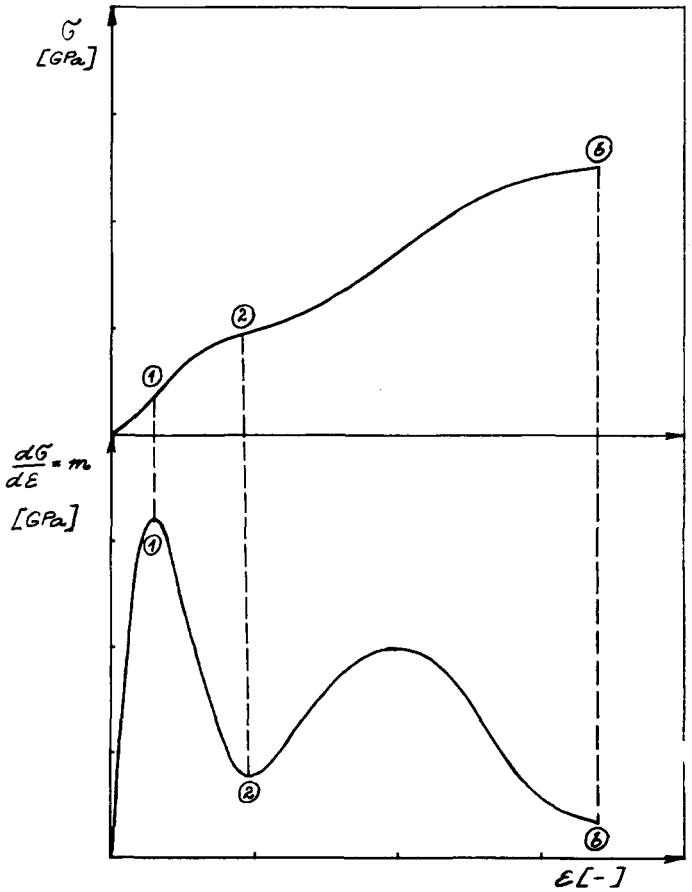

Fig. 1. Characteristic points on the stress–strain curve.

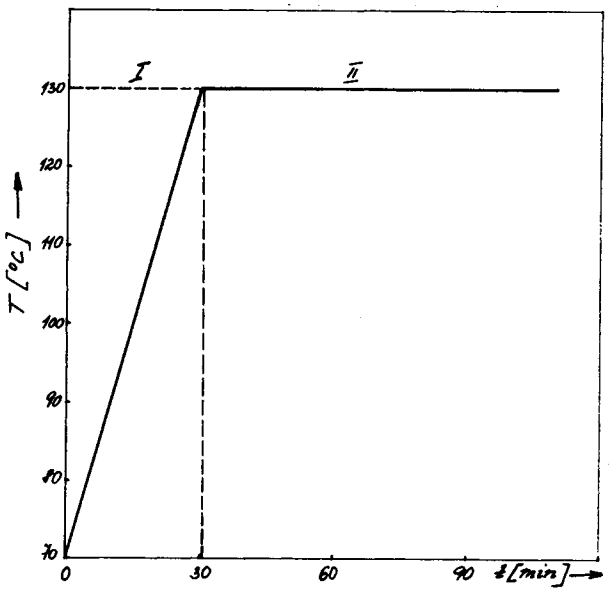

Fig. 2. Time-temperature course of dyeing.

dye concentration in the fiber was determined on the spectrophotometer from a monochlorobenzene extract. Baumgarte[12] gives a more detailed description of the procedure.

Modeling Nonisothermal Kinetics of Sorption

In modeling the kinetics of isothermal dyeing, Cegarra and Puente[13] started from the following assumptions:

(1) In the course of dyeing (especially in its initial phases), Fickean sorption of dye takes place represented by the linear relationship between dye concentration and the square root of time.

(2) Simultaneously with the Fickean sorption, partial desorption occurs, the rate of which is considered to be pseudomolecular.

The corresponding kinetic equation has the form

$$\frac{dC_t}{dt} = K\frac{C_\infty^2 - C_t^2}{C_t C_\infty^2} \tag{1}$$

where K is the rate constant, C_t is the mean dye concentration in the fiber at a time t, and C_∞ is the equilibrium mean dye concentration in the fiber. Under nonisothermal conditions K is a function of the sorption temperature T. Usually, the Arrhenius equation is chosen here,

$$K = K_\infty \exp(-\Delta E\#/RT) \tag{2}$$

where K_∞ is a preexponential factor proportional to the activation entropy, $\Delta E\#$ is the activation energy of sorption, and R is the gas constant. Substituting eq. (1) into eq. (2) and rearranging, we obtain

$$\int_0^C \frac{C_t C_\infty^2}{C_\infty^2 - C_t^2}\, dC_t = K_\infty \int_0^t \exp[-\Delta E\#/RT(\mathrm{t})]\, dt = F(T) \tag{3}$$

where $T(t)$ is the time–temperature course of sorption. The left-hand side of eq. (3) may be simply integrated. Denoting the right-hand side of eq. (3) as $F(T)$, the following relationship is obtained:

$$C_t^2 = C_\infty^2 [1 - \exp(-F(T))] \tag{4}$$

In region I of Figure 2, the temperature increases linearily with the time, i.e.,

$$T = T_0 + \theta t \tag{5}$$

where T_0 is the initial dyeing temperature and θ the rate of heating. $F(T)$ may be described as follows:

$$F_I(T) = \frac{2K_\infty}{C_\infty^2 \theta} \int_{T_0}^{T} \exp(-\Delta E\#/R\tau)\, d\tau \tag{6}$$

In region II of Figure 2, the temperature is a constant ($T = T_1$). $F(t)$ is expressed by

$$F_{II(T_1)} = \frac{2K_\infty}{C_\infty^2 \theta} \int_{T_0}^{1} \exp(-\Delta E\#/R\tau)\, d\tau + \frac{2K_\infty}{C_\infty^2} \exp(-\Delta E\#/RT_1)(t - t_1) \tag{7}$$

Equations (4), (6), and (7) define the resulting model equations describing nonisothermal dyeing kinetics. They contain only three model parameters, C_∞, K_∞, and $\Delta E\#$. These parameters may be assessed from experimental nonisothermal sorption curves by means of nonlinear regression. The whole problem is rather complicated by the need of integrating eqs. (6) and (7) in each iteration step. For this reason a program for HP 9825 desk-top computer was constructed based on an optimization of nonderivative procedure. Numerical integration is performed using Simpson's rule in 50 steps.

RESULTS

Table I shows the characteristics of individual fibers. In Table II, their structural parameters are given. These parameters determined on the fibers after dyeing in the blank dye bath under equal conditions are presented in Table III. Table IV shows the mechanical characteristics of the original samples, and Table V shows these characteristics after simulated dyeing in a blank bath. Corresponding stress–strain curves of individual fibers are illustrated in Figures 3(a) and 3(b); Figures 4(a) and 4(b) show the same curves for fibers dyed in the

TABLE I
The Characteristics of Individual Fibers

Sample no.	Draw ratio	DEG content, wt %
I-1	1:4.95	0.87
II-1	1:4.73	1.17
III-1	1:4.86	3.05
I-2	1:4.53	0.87
II-2	1:4.40	1.17
III-2	1:4.48	3.05

TABLE II
Structural Parameters of Fibers before Dyeing

Sample no.	T_m, °C	T_{rc}, °C	X	$\Delta n \times 10^{-3}$	f_c	f_{am}
I-1	256.0	149.2	0.31	184.16	0.887	0.652
II-1	255.0	147.9	0.34	185.88	0.882	0.661
III-1	247.7	148.0	0.31	185.90	0.922	0.649
I-2	257.0	146.1	0.33	184.30	0.889	0.649
II-2	254.8	145.1	0.31	185.73	0.915	0.650
III-2	247.9	147.0	0.31	177.63	0.888	0.591

blank bath. Table IV brings the model parameters of nonisothermal dyeing kinetics expressed by eqs. (4), (6), and (7) that were calculated by means of nonlinear regression with least-squares criterion. Since there is a functional dependence between the quantities $\Delta E\#$ and K_∞, [eq. (2)], they cannot be considered separately. That is why rate constants K_{130} for 130°C were computed. The resulting model curves describing experimental points with deviation of less than 3% are illustrated in Figure 5 for higher draw ratio and in Figure 6 for lower draw ratio.

DISCUSSION

From Table II it may be seen that no influence of the DEG content can be demonstrated on either the overall orientation or that of individual phases. The orientation is primarily a function of draw conditions and preorientation of the fibers. A small change of the draw ratio produces practically no effect on orientation of individual phases. The only change observable is that f_{am} slightly increases with increasing draw ratio. Table IV shows that increased DEG content reduces the stress at break point as well as the deformation work, simultaneously increasing the strain. Furthermore, T_m decreases as well. This is due to increase of irregularities in the crystal lattice, which agrees with Flory's melting theory.[9] Changes of T_{rc} are small, as we stated previously.[4] At both characteristic points on the stress–strain curves the stress σ, modulus m, and deformation work d decrease with increasing DEG content. Again, this may be explained by an increased number of defects in the microfibrillar structure of the

TABLE III
Structural Parameters of Fibers after Dyeing in Blank Bath

Sample no.	T_m, °C	T_{rc}, °C	X	$\Delta n \times 10^{-3}$	f_c	f_{am}
I-1	251.5	158.3	0.360	183.80	0.898	0.640
II-1	251.5	161.4	0.365	184.69	0.894	0.646
III-1	244.6	162.0	0.358	182.98	0.941	0.616
I-2	253.8	162.6	0.370	179.65	0.919	0.605
II-2	250.1	159.0	0.365	175.23	0.896	0.606
III-2	246.4	161.0	0.358	178.71	0.895	0.613

TABLE IV
Mechanical Characteristics of Fibers before Dyeing

Sample no.	ϵ_1	σ_1, GPa	m_1, GPa	$d_1 \times 10^{-4}$, J	ϵ_2	σ_2, GPa	m_2, GPa	$d_2 \times 10^{-4}$, J	σ_b, GPa	ϵ_b	$d_b \times 10^{-4}$, J
I-1	0.01	0.065	6.436	0.01	0.055	0.165	0.486	0.221	0.569	0.597	8.163
II-1	0.01	0.0597	6.025	0.0101	0.06	0.155	0.447	0.225	0.496	0.654	7.854
III-1	0.01	0.0647	5.649	0.0116	0.06	0.149	0.379	0.206	0.479	0.646	6.759
I-2	0.01	0.0686	6.282	0.0128	0.06	0.164	0.496	0.246	0.505	0.725	9.345
II-2	0.01	0.0639	6.074	0.0179	0.06	0.158	0.464	0.232	0.486	0.783	9.387
III-2	0.005	0.0402	5.752	0.00429	0.065	0.147	0.297	0.227	0.465	0.812	8.330

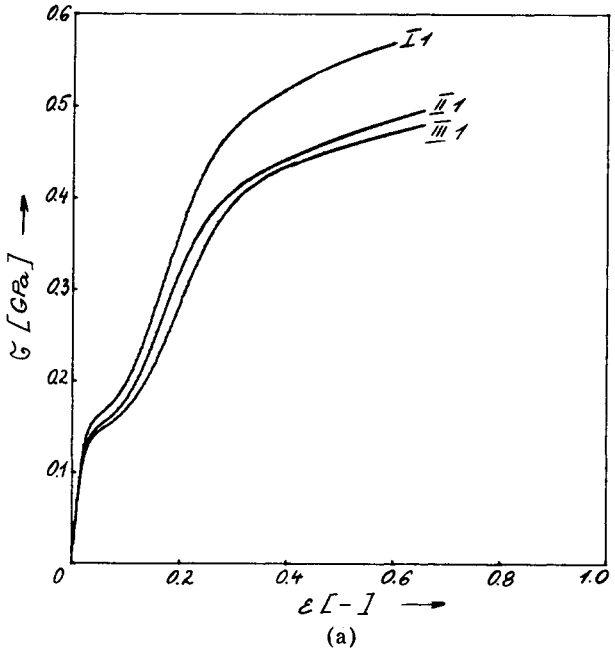

(a)

polymer (due to the presence of DEG copolymer). An apparent increase of sorption parameters, namely, C_∞ and K_{130}, can be explained with increased chain mobility in the amorphous phase. This is caused by the presence of more ali-

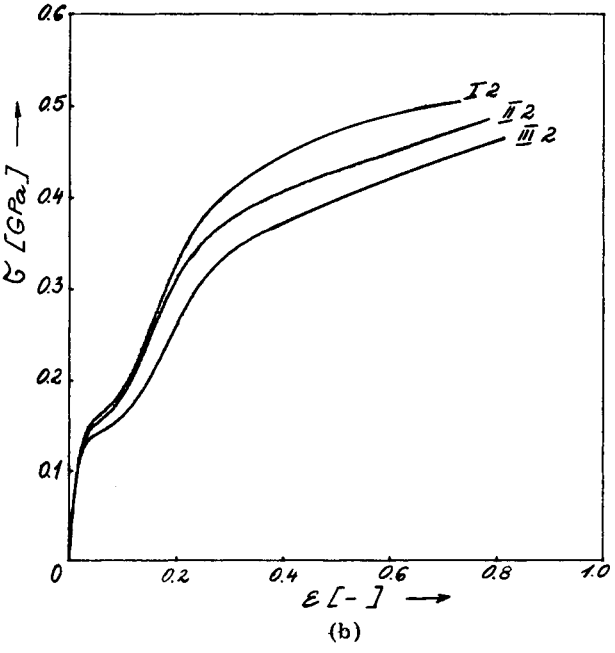

(b)

Fig. 3(a). Stress–strain curves of PET fibers (lower draw ratio). (3b) Stress–strain curves of PET fibers (lower draw ratio).

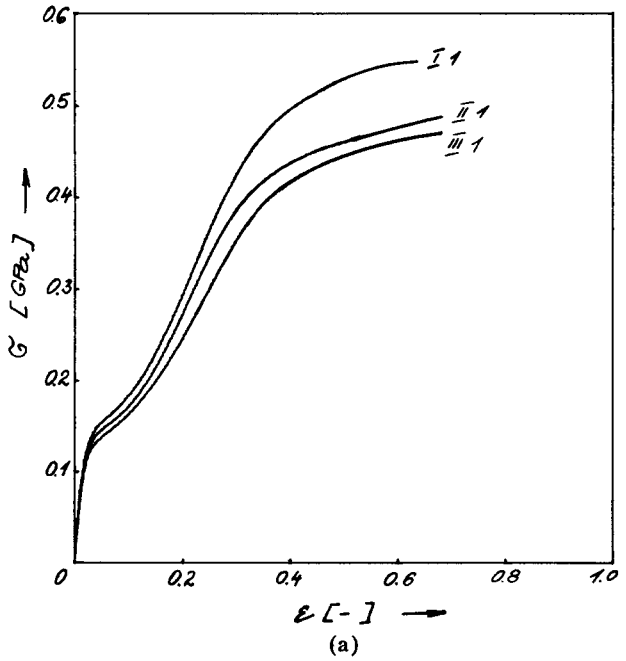

(a)

phatic flexible units in the PET chains. With increasing DEG content, activation energy and activation entropy of nonisothermal dyeing increase, too.

The draw ratio evokes an inverse effect on the chain mobility as well as the

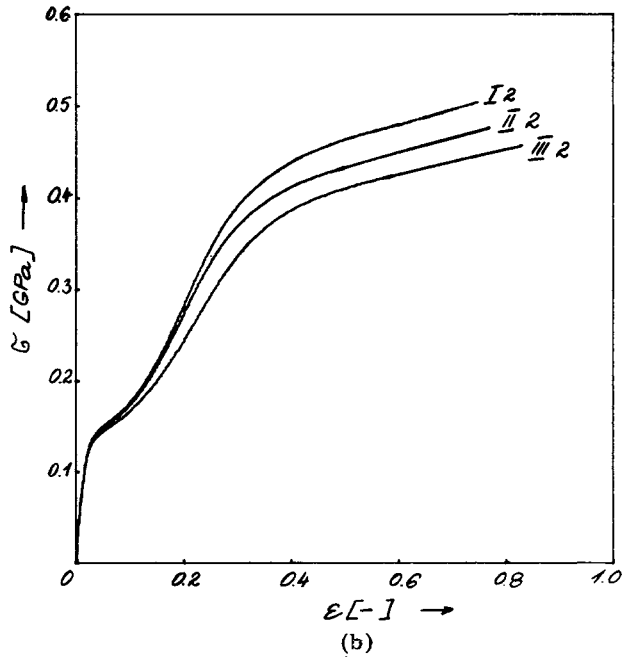

(b)

Fig. 4(a). Stress–strain curves of PET fibers after dyeing in blank dye bath (higher draw ratio). (b) Stress–strain curves of PET fibers after dyeing in blank dye bath (lower draw ratio).

TABLE V
Mechanical Characteristics of Fibers after Dyeing in Blank Bath

Sample no.	ϵ_1	σ_1, GPa	m_1, GPa	$d_1 \times 10^{-4}$, J	ϵ_2	σ_2, GPa	m_2, GPa	$d_2 \times 10^{-4}$, J	σ_b, GPa	ϵ_b	$d_b \times 10^{-4}$, J
I-1	0.01	0.0699	6.075	0.0136	0.060	0.159	0.502	0.242	0.548	0.634	8.229
II-1	0.01	0.0636	5.884	0.0120	0.065	0.153	0.445	0.248	0.488	0.678	7.916
III-1	0.01	0.0616	5.699	0.0106	0.060	0.135	0.434	0.195	0.470	0.680	7.038
I-2	0.01	0.0679	5.977	0.0130	0.065	0.157	0.443	0.263	0.504	0.747	9.353
II-2	0.01	0.0660	5.911	0.0125	0.065	0.155	0.442	0.253	0.477	0.767	9.040
III-2	0.01	0.0656	5.656	0.0117	0.065	0.150	0.411	0.229	0.458	0.827	8.619

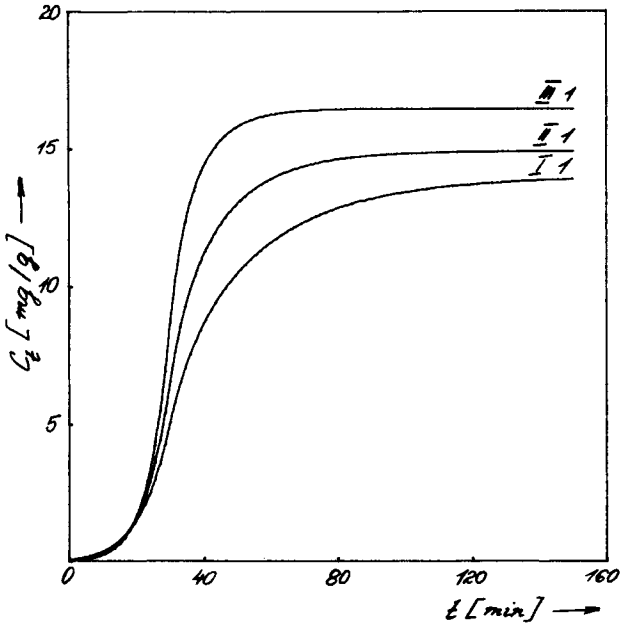

Fig. 5. Nonisothermal sorption curves of Disperse Blue 128 in PET fibers (higher draw ratio).

orientation degree in amorphous regions. Considering that no increase in crystallinity has been proved, the reduced mobility of the amorphous phase is due to increased draw ratio (indicated by higher T_{rc}[4]) and increased orientation function of the amorphous phase. Thus, we can say that the decrease in draw ratio has a similar effect as the addition of DEG.

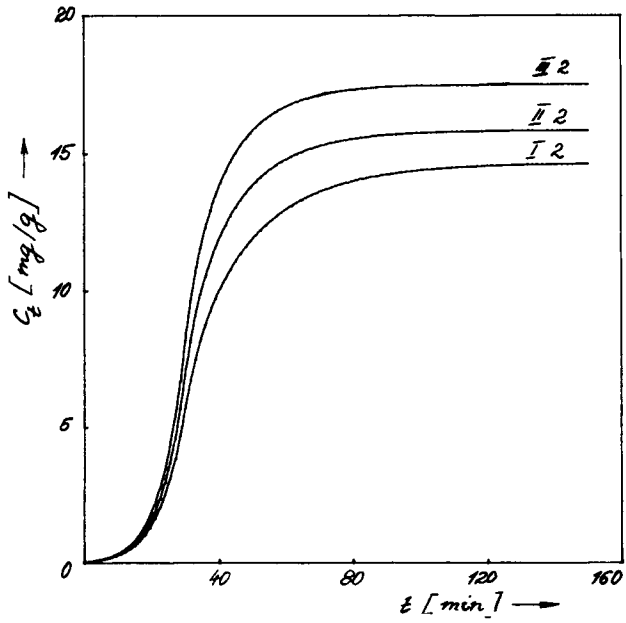

Fig. 6. Nonisothermal sorption curves of Disperse Blue 128 in PET fibers (lower draw ratio).

TABLE VI
Model Parameters of Nonisothermal Kinetics of Dyeing

Sample no.	C_∞, mg/g	$\Delta E\#$, kJ/mole	K_∞, min^{-1}	$K_{130} \times 10^{-2}$, min^{-1}
I-1	14.020	157.735	$9.366 \cdot 10^{20}$	3.47
II-1	14.937	182.635	$3.185 \cdot 10^{24}$	6.20
III-1	16.492	221.505	$7.737 \cdot 10^{29}$	10.90
I-2	14.670	180.273	$1.150 \cdot 10^{24}$	4.69
II-2	15.850	188.725	$2.250 \cdot 10^{25}$	6.29
III-2	17.510	191.155	$6.679 \cdot 10^{25}$	7.42

From what has been said it follows that sorption properties are connected with the chain mobility in the amorphous regions. The mobility is affected (a) in a positive sense by the presence of more flexible chains in noncrystalline regions (due to the DEG content); (b) in a negative sense by increase of orientation of the chains in the amorphous phase (expressed by increase in f_{am}). From this viewpoint, increased dyeability may be achieved either by reducing orientation of amorphous regions or increasing the number of flexible units.

As a consequence of simulated dyeing in the blank dye bath, the increase in crystallinity took place together with a decrease in orientation in the amorphous phase. The melting point decrease is probably due to disorientation of PET chains. Increased temperature of apparent setting indicates that temperature treatment in the dye bath (water at 130°C) exceeded the effect of the original annealing (in air at 130°C). After dyeing in the blank dye bath, stress at break decreases and strain increases with deformation work. At the point corresponding to the postyield point, the stress decreases and deformation work increases in most cases. However, at the point representing the end of pseudo-Hookean deformation, both stress and deformation work increase. The changes in modulus are more scattered.

It is obvious that the effect of the dye bath is complex. Thermal treatment combined with the diffusion of blank dye bath solution causes a crystallinity increase and an orientation decrease in the amorphous regions of the fiber. This would also explain the decrease of stress at break and increase of the corresponding strain.

It is interesting that after dyeing had been accomplished, stress σ_1 increased and, simultaneously, σ_2 decreased (points 1 and 2 in Fig. 1, respectively). Presumably, this is caused by an increase in the crystallinity with decreasing orientation in the amorphous regions.

CONCLUSIONS

The effect of DEG addition on the structure, mechanical properties, and sorption behavior of PET fibers has been investigated. It was found that diethylene glycol acts as a comonomer. This has been demonstrated on stress decrease at break point and increase of corresponding strain. Due to increased flexibility and, consequently, mobility of chains in the amorphous regions, the dyeing rate increases with increasing content of DEG. Moreover, equilibrium quantity of dye in the fiber increases as well. This means that in practice nonuniformity in dyeing, attributed hitherto only to fluctuation of draw ratio

and annealing temperature, can be caused by uncontrolled fluctuations in DEG content.

The authors are grateful to Dr. Ludvík Koukol of Chemopetrol Silon Combine for his generous help with the x-ray experimentation.

List of Symbols

C_t mean dye concentration in the fiber at time t
C_∞ equilibrium mean dye concentration in the fiber
ΔE activation energy of sorption
$F(t)$ symbolic expression for integral in eq. (3)
f_{am} orientation factor of amorphous phase
f_c orientation factor of crystalline phase
K_∞ preexponential factor
K rate constant
Δn birefringence
$\Delta^0 n_c$ intrinsic birefringence of crystalline phase
$\Delta^0 n_{am}$ intrinsic birefringence of amorphous phase
R gas constant
T temperature
T_0 initial dyeing temperature
T_1 temperature in the isothermal part of time–temperature course of sorption
$T(t)$ time–temperature course of sorption
T_m melting temperature
T_{rc} apparent temperature of setting
X volumetric degree of crystallinity
ρ_{am} density of amorphous phase
ρ_c density of crystalline phase
θ heating rate
τ integration variable
d_i deformation work at point i on stress–strain curve
m_i tensile modulus at point i on stress–strain curve
ϵ_i tensile strain at point i on stress–strain curve
σ_i tensile stress at point i on stress–strain curve, where $i = 1$ in end of pseudo-Hookean region of deformation, $i = 2$ in the postyield point, and $i = b$ is the breaking point

References

1. R. McGregor and R. H. Peters, *J. Soc. Dyers Colour,* **84,** 267 (1968).
2. V. B. Gupta and G. R. Sudarskana, *J. Appl. Polym. Sci.,* **20,** 345 (1976).
3. H. Berg, *Melliand Textilber,* **52,** 448 (1971).
4. J. Vaniček, *Thermal Analysis,* Vol. 3, Proceedings of the 4th ICTA, Budapest, Buzás, Ed., 1974, Akademia Kiado, Budapest, 1975.
5. R. P. Daubrey, C. W. Bunn, and C. J. Brown, *Proc. Roy. Soc. London Ser. A,* **226,** 531 (1954).
6. S. W. Lasoski and W. H. Cobbs, *J. Polym. Sci.,* **36,** 21 (1959).
7. P. H. Hermans and P. Platzek, *Kolloid Z.,* **89,** 68 (1939).
8. J. Militký, J. Dostál, and J. Burešová, Proceedings of the XIIIth Conference of Synthetic Fibers, České Budějovice, May 1978.
9. P. J. Flory, *J. Chem. Phys.,* **17,** 223 (1949).
10. J. U. Dumbleton, *J. Polym. Sci. Part A2,* **6,** 667 (1968).

11. R. M. Samuels, *J. Polym. Sci. Part A,* **3,** 1741 (1965).
12. M. Baumgarte, *Melliand Textilber,* **53,** 790 (1973).
13. J. Cegarra and P. Puente, *Text. Res. J.* **37,** 343 (1967).
14. J. Militký, Non-isothermal Kinetics of Dyeing, Res. Report No. 6, 1978, VUZ Dvůr Králové, September 1978.
15. J. B. Kirby, A. J. Baldwin, and R. H. Heidner, *Anal. Chem.,* **37,** 1306 (1965).
16. S. G. Hovenkamp and J. P. Munting, *J. Polym. Sci. Part A1,* **8,** 678 (1970).
17. J. Militký, *Czech Textile,* to appear.
18. J. Militký, J. Vaníček, and J. Dostál, IUPAC Conference on Macromolecular Chemistry, Taskent, October 1978 (Poster No. 237).
19. M. Hoffmann and J. Jansa, *Melliand Textilber,* **53,** 259 (1972).
20. J. H. Dumbleton, J. P. Bell, and T. Murayma, *J. Appl. Polym. Sci.,* **12,** 2491 (1968).
21. R. H. Peters and W. Ingamells, *J.S.D.C.,* **91,** 937 (1975).
22. J. J. Donze, G. Bouchet, R. Freytag, J. Chabert, R. Scheider, and P. Viallier, *J.S.D.C.,* **91,** 336 (1975).
23. J. Vaníček, J. Militký, J. Dostál, J. Šrůta, and L. Koukol, Influence of Technological Parameters on Dyeability of Pet Fibres, Res. Report No. 146, Silon, Planá n. Luž, October 1977.

Received January 19, 1979
Revised October 10, 1979